

Detection of induction motor broken bars in grid and frequency converter supply

Abstract. This paper presents the experimental study of three-phase squirrel cage induction motor broken rotor bars diagnostics. Tests have been performed with two different machines, one through a frequency converter and the other supplied directly from grid. This comparison has been presented, as the use of frequency converters changes the traditional current spectrum of the machine and hence the diagnostic of such machines becomes more difficult. Necessity for further study on the behavior of the frequency converter in the weak grid is pointed out.

Streszczenie. W artykule zaprezentowano metodę diagnostyki trójfazowego silnika indukcyjnego z uszkodzonymi prętami. Zaprezentowano widmo sygnału prądowego różnych silników. (Wykrywanie uszkodzonych prętów silnika indukcyjnego na podstawie widma częstotliwościowego prądu)

Keywords: condition monitoring, frequency converter, electric machines, induction motors.

Słowa kluczowe: diagnostyka silnika indukcyjnego, widmo częstotliwościowe.

doi:10.12915/pe.2014.01.22

Introduction

Induction machines are by far the most widely industrial electrical machine type in nowadays world and considering their rugged build and cost-efficiency, their popularity can be expected to stay the same if not increase in the near future. In fact, in developed countries today there are more than 3 kW of electric motors per person and most of it is from induction motors [1]. Failures and faults in such machines can often have dramatic results and pose danger for the people and surroundings and cause economic problems for the industries, whose production depends on them.

The majority of all stator and rotor faults are caused by a combination of various stresses, which can be thermal, electromagnetic, residual, dynamic, mechanical or environmental [2]. These stresses can cause a number of different failures in electrical machines. In the case of squirrel cage induction machines, one of the most common faults is the cracking and eventually breaking of rotor bars. The main concern regarding such faults is that it is often not worth or possible to repair the rotor, if the fault has been detected too late. However all of this can be avoided, when the motor is supervised by an appropriate condition monitoring or diagnostic system allowing the anticipation of the fault and its propagation.

With the development of power electronics, many machines are today supplied by frequency converters, which enables good control of the torque and speed and thus energy saving in ,e.g., pumping and ventilation applications. However, the frequency converter supply changes the natural and traditional current spectrum of electrical machines. This also means that diagnostic measures have to be changed to match the peculiarities in the behavior of electrical machines connected to converters. However, the main requirements for diagnostic methods still stay the same, such as no additional changes or disturbances to the working cycle of the machines, when performing condition monitoring.

This paper describes an experimental study where broken rotor bars diagnostics of induction motor is performed on a machine that is supplied directly from grid and also a machine that is driven through a frequency converter. The studied parameters are the motor terminal currents and voltages. The first part of the paper describes the measurement set up and the following parts reviews the Clarke's vector equations and analyzes the measurements based on these equations.

Measurements

Measurements described in this paper were performed in two separate series. For the experiments, where the induction motor is supplied straight from the grid, a motor with a healthy rotor and a rotor with seven broken bars was used. In the experiments with supply through a frequency converter, a motor with a healthy rotor and a rotor with three broken bars was used. Broken rotor bars were situated next to each other in both cases. Schematics of the setups for the tests are presented in Fig. 1.

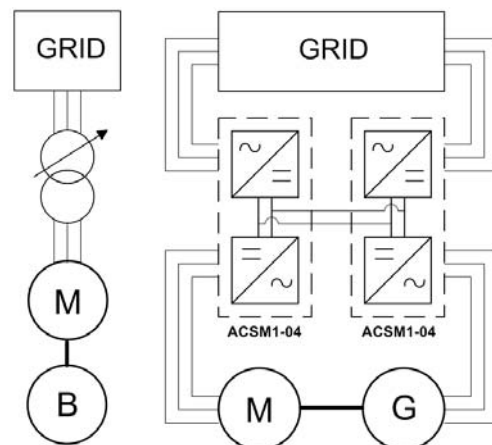


Fig.1. Schematics of experimental setups used for testing. Left – motor is fed directly from the grid through an autotransformer and loaded with an electromagnetic brake; right – motor is fed through frequency converters and loaded by an identical motor and frequency converter in regeneration mode.

In case of Motor 1, the machine is supplied directly from the grid through an autotransformer. The motor is loaded using an electromagnetic brake. Tested induction machine was connected in star during the tests.

Motor 2 is supplied from the grid through ABB ACSM1-04 frequency converters. Scalar control was used for driving the machine. Motor was loaded using an identical machine in generator mode and the machine was also connected to star during the testing period. The DC-links of the frequency converters were connected in parallel and only the power losses from both machines and frequency converters were drawn from the grid. Table 1 presents more precise data of the tested induction motors.

Table 1. Technical data of the tested induction motors

Parameter	Symbol	Motor 1	Motor 2
		Value	Value
Rated voltage	U_n	177 V	380-415 V
Rated current	I_n	14.8 A	41 A
Rated speed	n_n	1456 rpm	1700 rpm
Rated power	P_n	3 kW	22 kW
Frequency	f	50 Hz	60 Hz
Power factor	$\cos\varphi$	0.785	0.860
Number of poles	p	4	4
Number of rotor bars	Q_r	44	40
Number of stator slots	Q_s	36	48

Analysis and discussion

Clarke's vector approach is an easy way to decide if the motor is healthy or not [5]. It means that the phase currents (i_a, i_b, i_c) are transformed to current alpha and beta components (i_α, i_β) and placed on α -axis and β -axis respectively. In other words, a three-dimensional system is transformed to a two-dimensional one assuming the zero component of the space vector is not allowed to flow, which holds true in case of star connection of the machine. The two components of the Clarke's current vector are then given as:

$$(1) \quad \begin{cases} i_\alpha = i_a \\ i_\beta = \frac{1}{\sqrt{3}}(2i_b + i_c) \end{cases}$$

Its representation at steady state operation of the machine is a circular pattern centered at the origin of the $\alpha\beta$ -coordinate system. This is a very simple reference figure, which allows the detection of an abnormal condition due to any fault of the machine by observing the deviations of the acquired picture from the reference pattern [6].

The healthy pattern differs slightly from the expected circular one, because of the distortion and unbalance of the supply voltage and thus of the current space vector [7]. Clarke's vector current pattern of the rotor with broken bars is however more ellipse-shaped and its discrepancy from the circular pattern could be used for fault detection [8].

The Clarke's vector can be also used to transform the three-phase voltages at the terminal of the machine into α - and β -axis components:

$$(2) \quad \begin{cases} u_\alpha = u_a \\ u_\beta = \frac{1}{\sqrt{3}}(2u_b + u_c) \end{cases}$$

where $u_a, u_b,$ and u_c are the phase voltages and u_α, u_β are the voltage alpha and beta components. This gives the opportunity to monitor the stator voltage as well as current and make the decisions upon the analyses of the obtained graphs [6].

Using Park's vector (and also Clarke's vector) approach for diagnostic purposes of electrical machines is not a novel idea itself. It has been proposed in the end of 80's by Cardoso et al [9]-[11], however, the method did not become widely used as there were significant doubts on the automation possibilities of the process. Nowadays, when computation technologies have advanced, the method can be implemented far more easily, e.g., with pattern recognition algorithms [12]. In addition, usage of Clarke's vector approach on stator voltage instead of current will

grant a wider segment of possible diagnostic usage as the supply voltage of electrical machines is generally held at a constant value and is not much affected by the scalar control, which is by far the most used control methodology in applications with less requirements on the dynamic behavior of the drive system.

Grid operation (Motor 1)

In the tests with direct grid supply, the induction motor with a healthy rotor and a rotor with seven broken bars was used. All the broken rotor bars were situated next to each other, as it is the most probable case in practice and the asymmetry in such case is more severe. It should be noted that Motor 1 has die-cast aluminum cage, which is prone to bad casting and thus could present several broken bars not only at operation but right away after the manufacturing process. MATLAB software was used to analyze the data.

If one looks at the presented figures (Figs. 2-9), it can be observed that there are some unexpected curves and declinations from the expected vector pattern. This is caused mainly by the supply voltage used during the tests. As the supply was not exactly sinusoidal, the deviations from ideal sinusoid can also be traced in the resulting figures. However, this phenomenon can be left aside, as the healthy and faulty conditions of the motor are clearly visible from the figures regardless of the imperfection in the supply.

First two figures (Figs. 2 and 3) show Clarke's vector pattern of the stator current while the machine is working at no load conditions.

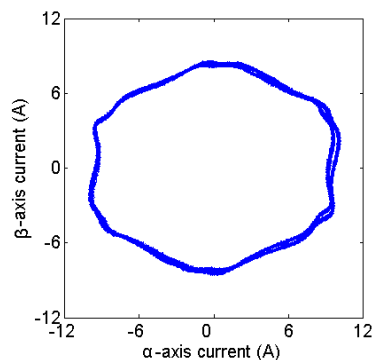


Fig.2. Stator current Clarke's vector pattern of healthy motor at no load conditions (Motor 1)

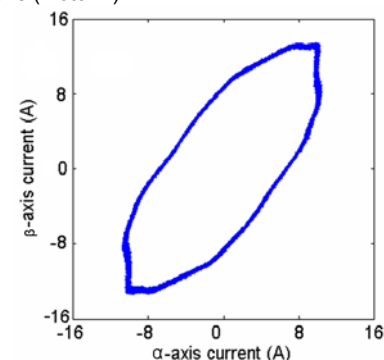


Fig.3. Stator current Clarke's vector pattern of faulty motor at no load conditions (Motor 1)

As the figures show, the healthy motor Clarke's vector current pattern has indeed a more or less circular shape and the faulty one looks more close to an ellipse as referred to in the literature [9]. In addition, it was found that the absolute value of current is higher in the case of faulty motor, which was also expected prior to the testing.

Next figures (Figs. 4 and 5) are showing the machine at rated torque conditions.

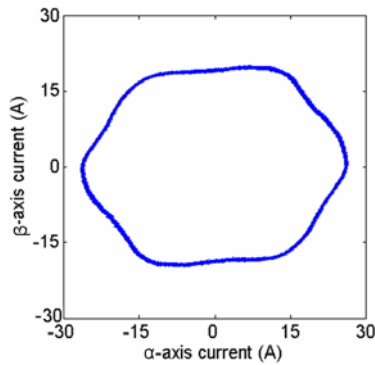


Fig.4. Stator current Clarke's vector pattern of healthy motor at full load conditions (Motor 1)

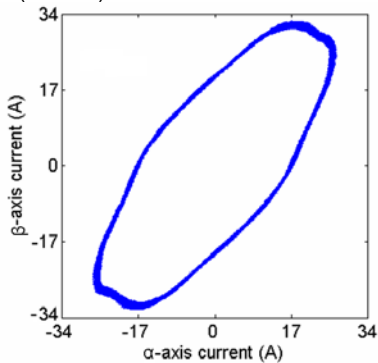


Fig.5. Stator current Clarke's vector pattern of faulty motor at full load conditions (Motor 1)

Faulty case can be traced easily in the full load figures as well, due to the major differences in the pattern shape of healthy and faulty conditions. If one compares the figures of no load and full load operations, it can also be clearly seen that the current amplitude rises as more torque is applied to the machine.

Next figures (Figs. 6 and 7) are plotted using the Clarke's vector approach on stator voltage at the same time moment as the current data was gathered. Usage of stator voltage should yield better results and no load condition is observed first.

The figures show that the voltage pattern of the healthy motor looks again more as a circle and that of the faulty motor more like an ellipse. Such a dramatic change would not be expected if the supply network was enough rigid to withstand to effect of fault in the motor. Furthermore, changes in scale are more drastic and better traceable in case of the voltage graphs. Additionally, from the healthy case graph it can be seen that deviations due to the non-ideal sine voltage supply are not so vivid in the voltage case.

Figs. 8 and 9 are from the full load test, again taken in the same time moment as for the current figures.

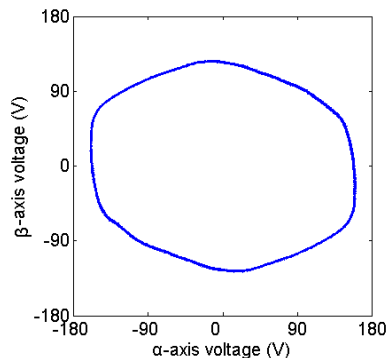


Fig.6. Stator voltage Clarke's vector pattern of healthy motor at no load conditions (Motor 1)

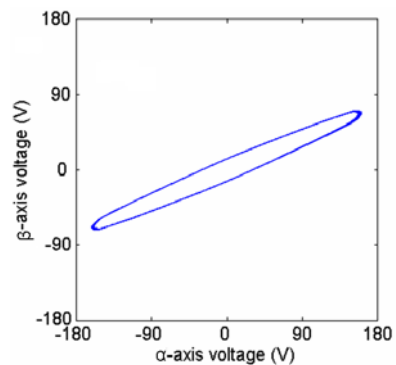


Fig.7. Stator voltage Clarke's vector pattern of faulty motor at no load conditions (Motor 1)

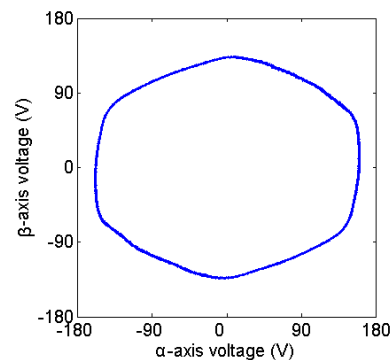


Fig.8. Stator voltage Clarke's vector pattern of healthy motor at full load conditions (Motor 1)

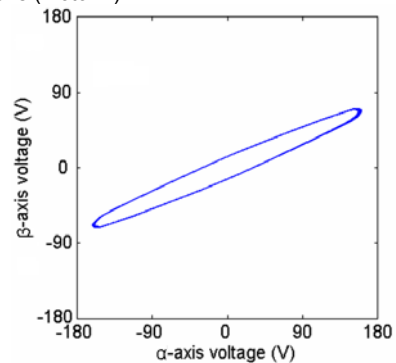


Fig.9. Stator voltage Clarke's vector pattern of faulty motor at full load conditions (Motor 1)

When no load situation and full load situation are compared, it can be seen that they match in to a very large extend, which means that most of the changes in the patterns are due to the voltage unbalance caused by the seven broken rotor bars in the induction motor and not any other deviations in the grid or other variables.

Frequency converter operation (Motor 2)

A three-phase squirrel cage induction motor with a healthy rotor and a rotor with three broken bars situated next to each other was used for performing these tests. The machine was not supplied directly from grid but through a frequency converter using scalar control instead.

It is a commonly known fact that faults such as the broken rotor bars induce sideband harmonic components to the stator current spectrum of the induction motor. Those harmonics are used as fault indicators in the diagnostic process. Frequency converter causes supply frequency to slightly vary in time and, as a result, some additional harmonics in the current spectrum are induced and sidebands are reduced [13]. Depending on the type of the frequency converter the damping of sideband frequencies can be varying in a very large scale due to the raised

amount of noise in the test signals, which makes the faults more difficult to detect.

In the tests with frequency converters both current and voltage changes are observed as they were in the tests with direct grid supply. Figs. 10 and 11 present stator current Clarke's vector patterns of healthy and faulty cases under no load conditions.

If the figures of different cases are compared, no large scale changes can be detected as it was in the case with the grid supplied machine. Main difference compared to previous figures is the thicker line of the vector pattern, which is caused by the slightly changing supply frequency of the used frequency converter. As the supply frequency changes, it causes a slight change in the trajectory of the Clarke's vector and thus the vector pattern line becomes thicker.

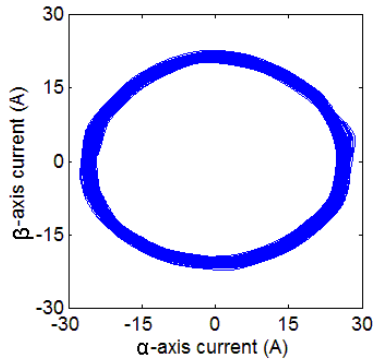


Fig. 10. Stator current Clarke's vector pattern of healthy motor at no load conditions (Motor 2)

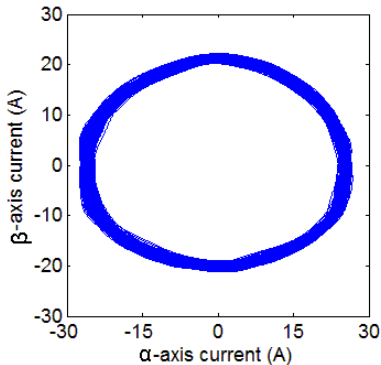


Fig. 11. Stator current Clarke's vector pattern of faulty motor at no load conditions (Motor 2)

Next figures (Figs. 12 and 13) describe stator current Clarke's vector pattern of both healthy and faulty cases on nominal load operation.

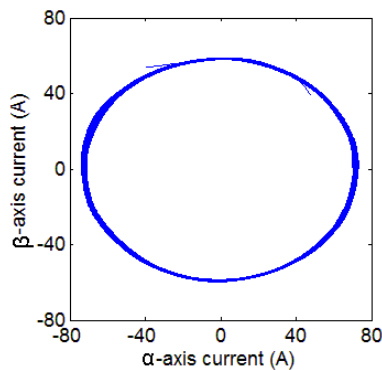


Fig. 12. Stator current Clarke's vector pattern of healthy motor at full load conditions (Motor 2)

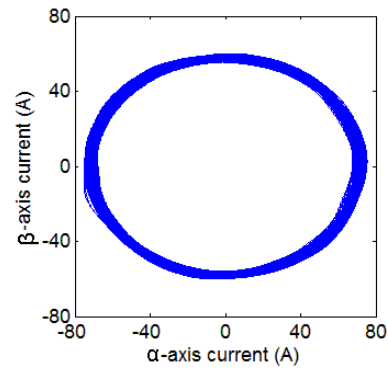


Fig. 13. Stator current Clarke's vector pattern of faulty motor at full load conditions (Motor 2)

Those figures again do not show as large changes as it could be expected from the grid operation tests. Some change in the thickness of the stator current pattern can be observed, but change of shape is minuscule. The detection of the fault however is very complicated if not impossible when analyzing the stator current pattern of the machine equipped with a frequency converter. It can be said that it is very complicated to differentiate the faulty rotor from the healthy rotor in the case where induction motor is used with a frequency converter. As usage of voltage gave some benefits in the grid operation tests, it can be expected also when frequency converters are used. No load tests in such case are presented in Figs. 14 and 15.

As expected, the differences are more traceable when stator voltage pattern analysis is used. However, the signals are very noisy due to the additional harmonic components induced by the converter. Again the trajectory of the vector pattern is wider, which results in a thicker pattern line, but results are better and allow differentiation of the faulty case.

Last figures (Figs. 16 and 17) present the stator voltage Clarke's vector pattern under full load conditions.

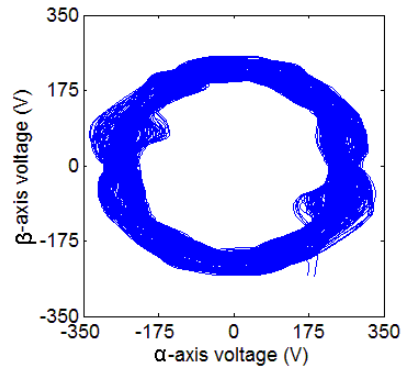


Fig. 14. Stator voltage Clarke's vector pattern of healthy motor at no load conditions (Motor 2)

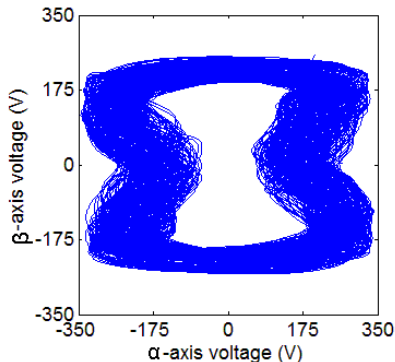


Fig. 15. Stator voltage Clarke's vector pattern of faulty motor at no load conditions (Motor 2)

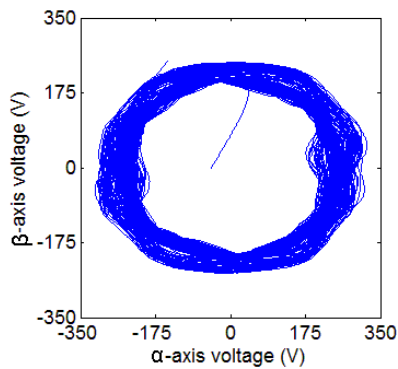


Fig. 16. Stator voltage Clarke's vector pattern of healthy motor at full load conditions (Motor 2)

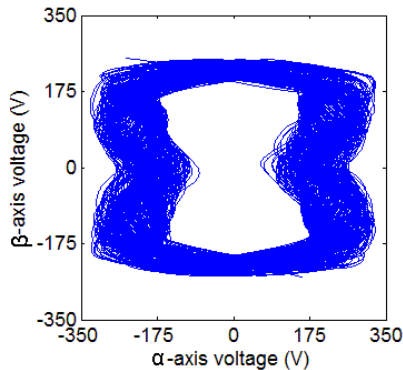


Fig. 17. Stator voltage Clarke's vector pattern of faulty motor at full load conditions (Motor 2)

Both full load and no load figures are very similar to each other. The faulty case does not look like an ellipse, as it could be expected and this can be related to the switching frequencies, additional harmonics and varying supply frequency caused by the converter. It should be noted that the filtration level during the analysis of the result has been kept the same both in grid and frequency converter operation figures. Nevertheless, as the changes in the pattern shapes are clearly visible, it means that analysis of stator voltage in case of broken bars of the frequency converter driven induction motor can be used more effectively for determination of the rotor fault than the analysis of stator current [14].

Conclusion

Conducted experiments and analyses show that although traditionally used for transformation of current data, Clarke's vector approach can be very effectively used for transformation of three-phase voltage. For diagnostic purposes this might be a better use of the method, as supply voltage of electrical machines is generally held at a constant value. Also using voltage as a diagnostic parameter will gain a wider range of possible setups that can be monitored as scalar control and load conditions do not affect the voltage pattern. This peculiarity of voltage patterns gives the opportunity for better and more precise decisions as healthy and faulty case data can be compared without any changes or recalculations of amplitudes.

Frequency converters, due to slightly time-varying supply frequency, induce additional harmonics to the current spectrum of the machines, which reduces or even hinders the sideband frequencies that are used as fault indicators. Also they create more noise in the signals, which makes detection of the fault more complicated. As seen from the figures, presented in this paper, current pattern cannot be used for diagnostic purposes as the fault

indicators are not visible, which is not the case when voltage is used.

When diagnostics via the comparison of induction motor performance models is desired, the described method could be used in a sufficiently effective way to decide upon the state of the motor [13]. This can be automated using various algorithms and thus would be an effective way of diagnostics, which does not need vast computational resources due to the simplicity of the mathematical model. The model or figure of the healthy case of the motor can be used as a master model, to which other graphs would be compared to. It could prove to be a very good way for performing diagnostics also in the sense that no disturbance in the working cycle of the motor is needed in order to perform the needed measurements and analysis. The method could also be for testing the success of die cast aluminum cages of low power motors.

REFERENCES

- [1] Boldea I., Nasar S., The Induction Machine Handbook. Boca Raton: CRC Press, (2002), 950
- [2] Bonnett, A., Soukup, G., Cause and Analysis of Stator and Rotor Failures in Three-Phase Squirrel-Cage Induction Motor, *IEEE Trans. Ind. Appl.*, 28 (1992), No.5, 921-937
- [3] Vaimann, T., Kallaste, A., Kilk, A., Using analysis of stator current for squirrel-cage induction motor rotor faults diagnostics, in *Proc. ECT 2011*, (2011), 245-251
- [4] Vaimann, T., Kallaste, A., Kilk, A., Sensorless detection of induction motor rotor faults using the Clarke vector approach, *Scientific Journal of Riga Technical University*, 29 (2011), 43-48
- [5] Cardoso, A., Saraiva, E., Computer-aided detection of airgap eccentricity in operating three-phase induction motors by Park's vector approach, *IEEE Trans. Ind. Appl.*, 29 (1993), No. 3, 897-901
- [6] Vaimann, T., Kallaste, A., Kilk, A., Overview of sensorless diagnostic possibilities of induction motors with broken rotor bars, in *Proc. EPE 2011*, (2011), 183-186
- [7] Benbouzid, M., A review of induction motor signature analysis as a medium for faults detection, in *Proc. IEEE IECON 1998*, 4 (1998), 1908-1913
- [8] Miletic, A., Cettolo, M., Frequency converter influence on induction motor rotor faults detection using motor current signature analysis – experimental research, in *Proc. SDEMPED 2003*, (2003), 124-128
- [9] Cardoso, A., Saraiva, E., On-line diagnostics of three-phase induction motors, by Parks Vector, in *Proc. ICEM*, 1 (1988), 231-234
- [10] Cardoso, A., Saraiva, E., On-line diagnostics of current source inverter-fed induction machines, by Park's Vector Approach, in *Proc. ICEM*, (1990), 1000-1005
- [11] Cardoso, A., Cruz, S., Carvalho, J., Saraiva, E., Rotor Cage Fault Diagnosis in Three-phase Induction Motors, by Park's Vector Approach, in *Proc. IAC*, 1 (1995), 642-646
- [12] Amaral, T., Pires, V., Martins, J., Pires, A., Crisostomo, M., Image processing to a neuro-fuzzy classifier for detection and diagnosis of induction motor stator fault, in *Proc. IEEE IECON 2007*, (2007), 2408-2413
- [13] Vaimann, T., Belahcen, A., Martinez, J., Kilk, A., Detection of Broken Bars in Frequency Converter Fed Induction Motor Using Park's Vector Approach, in *Proc. PQ 2012*, (2012), 53-56
- [14] Vaimann, T., Kallaste, A., Kilk, A., Using Clarke Vector Approach for Stator Current and Voltage Analysis on Induction Motors with Broken Rotor Bars, *Electronics and Electrical Engineering*, 123 (2012), No. 7, 17-20

Authors: M.Sc. Toomas Vaimann, E-mail: toomas.vaimann@ttu.ee; prof. Anouar Belahcen, E-mail: anouar.belahcen@aalto.fi; M.Sc. Javier Martinez, E-mail: javier.martinez@aalto.fi; ass.prof. Aleksander Kilk, E-mail: aleksander.kilk@ttu.ee; Tallinn University of Technology, Department of Electrical Engineering, Ehitajate tee 5, 19086 Tallinn, Estonia; Aalto University, Department of Electrical Engineering, P.O. Box 13000, FI-00076 Aalto, Finland.